Dissolved major ions, Sr and $^{87}Sr/^{86}Sr$ of coastal lakes from Larsemann hills, East Antarctica: Solute sources and chemical weathering in a polar environment

Mohammad Nuruzzama*[1, 2], Waliur Rahaman[1], Gyana Ranjan Tripathy[3], Rahul Mohan[1], Shramik Patil[1]

[1] ESSO-National Centre for Polar and Ocean Research, Goa, India

[2]School of Earth, Ocean and Atmospheric Sciences, Goa University, Goa, India

[3]Department of Earth and Climate Science, Indian Institute of Science Education and Research, Pune – 411008, India

Key findings

1. Oceanic sources dominate (~80%) the water chemistry of coastal lakes from the Larsemann Hills, East Antarctica.
2. This study provides quantitative estimates of chemical weathering and CO_2 consumption rates in Antarctica and its global comparison.
3. Silicate weathering and CO_2 consumption rates in Antarctica are slightly lower (3.6 tons/km^2/yr and 0.5 x10^5 moles/km^2/yr respectively) than global river basins.
4. Present-day substantial weathering in these extreme cold climatic regime hints at its significant role in CO_2 budget during warmer periods in geological past.

This article has been accepted for publication and undergone full peer review but has not been through the copyediting, typesetting, pagination and proofreading process which may lead to differences between this version and the Version of Record. Please cite this article as doi: 10.1002/hyp.13734.

This article is protected by copyright. All rights reserved.

Accepted Article

Keywords: Coastal lakes, Antarctica, water chemistry; Sr isotopes, Glacial weathering; Inverse model.

Running head: Solute sources and chemical weathering in Antarctica

*Corresponding author: nuruzzama95@ncaor.gov.in
(mohammadnuruzzama@gmail.com)

Abstract

Dissolved major ions, Sr concentrations and $^{87}Sr/^{86}Sr$ ratios of ten coastal lakes from the Larsemann Hills, East Antarctica have been studied to constrain their solute sources, transport and glacial weathering patterns in their catchments. In absence of perennial river/streams, lakes serve as only reliable archive to study land surface processes in these low-temperature regions. The lake water chemistry is mostly Na-Cl type and it does not show any significant depth variations. Sr isotope compositions of these lakes vary from 0.7110 to 0.7211 with an average value of 0.7145, which is higher than modern seawater value. In addition to oceanic sources, major ions and Sr isotopic data show the appreciable amount of solute supply from chemical weathering of silicate rocks in lake catchments and dissolution of Ca-Mg rich salts produced during the freezing of seawaters. The role of sulphide oxidation and carbonate weathering are to be found minimal on lake hydro-chemistry in this part of Antarctica. Inverse model calculations using this chemical dataset provide first-order estimates of dissolved cations and Sr; they are mostly derived from oceanic (seawater + snow) sources (cations ~76%) and Sr ~92%)) with minimal supplies from weathering of silicates (cations ~15%); (Sr ~2%) and Ca-rich minerals (cations ~9%); Sr ~7%). The silicate weathering rate and its corresponding atmospheric CO_2 consumption rate estimates for Scandrett lake catchment (3.6 ± 0.3 tons/km^2/yr and 0.5 x10^5 moles/km^2/yr), are lower than

Accepted Article

This article is protected by copyright. All rights reserved.

that of reported values for the average global river basins (5.4 tons/km^2/yr and 0.9 x 10^5 tons/km^2/yr) respectively. The present study provides a comprehensive report of chemical weathering intensity and its role in atmospheric CO_2 consumption in low-temperature pristine environment of Antarctica. These estimates underscore the importance of Antarctica weathering on atmospheric CO_2 budget, particularly during the past warmer periods when the large area was exposed and available for intense chemical weathering.

Accepted Article

This article is protected by copyright. All rights reserved.

1. Introduction

Antarctica, the southernmost continent of the Earth, is mostly (~98% of its area) covered by ice with an average thickness of about 2 km (Fretwell et al., 2013; Morlighem et al., 2019). Chemical weathering processes in this vast continent and its role in solute supply to Antarctic lakes, surrounding oceans and atmospheric CO_2 consumptions could be important. Further, this cold and semi-arid desert could serve as a terrestrial analogue for the Martian surface, making it an ideal location to understand the land surface processes on Mars (Dickinson & Rosen, 2003; Gibson, Wentworth, & McKay 1983; Heldmann et al., 2013). The rock weathering in Antarctica is dominated by glacial/wind induced physical weathering (Campbell & Claridge, 1987; Robert & Kennett, 1997) and chemical rock-water interaction, mostly in the hyporheic zone of streams (Nezat, Lyons & Kathleen, 2001). The glacial action such as freeze-thaw cycle is considered as one of the strong agents of mechanical breakdown of rocks (Foster & Vance, 2006; Gibbs & Kump, 1994). Chemical weathering in this seasonal ice-free region is promoted by intense physical erosion due to waxing and waning of glacial ice sheets and frequent exposure of bedrock with fresh mineral surfaces. Available studies on the Antarctica weathering have reported that the weathering rates in these sub-zero temperature regions are comparable to that of the temperate rivers (Cuozzo et al., 2019; Lyons et al., 2015; Nezat et al. 2001). Hence, Antarctica weathering might have played significant role in regulating past global seawater chemistry during warmer conditions, when large areas of Antarctica was exposed (Zachos, Opdyke, Quinn, Jones, & Halliday, 1999). Despite its planetary and oceanographic significance, detailed investigations on the

Accepted Article

This article is protected by copyright. All rights reserved.

Antarctica weathering rates have been limited mainly due to remoteness and inaccessibility to the regions.

The ice-free areas of Antarctica mostly occur in coastal regions, which are relatively warmer than inland and receive significant amount of glacial melt-water input during the austral summer. Repeated waxing and waning of the glacial ice sheets and their movement caused strong physical erosion in the past, that lead to the formation of small to medium size depressions which eventually formed permanent lakes (Hodgson et al., 2012). In absence of perennial rivers/streams, these lakes are the only archive to study solute dynamics, biogeochemical cycling and on-going surficial process in Antarctica. A large numbers of surface and subglacial lakes (~10,000) have been reported from Antarctica, however, only a few of them have been studied to understand water chemistry and their solute sources (Lyons, Bullen, & Welch, 2017; Lyons et al., 2005; Lyons et al., 2003; Sabbe, Verleyen, Hodgson, Vanhoutte, & Vyverman, 2003). Multiple factors may contribute to the solute chemistry of these lakes which include chemical weathering of the bedrocks, biogeochemical processes, snow-ice melting, evaporation, precipitation, aerosol induced dust deposition, sea salt spray and anthropogenic activities (Sabbe et al., 2004; Verleyen et al., 2011; Wilson, 1979). Chemical weathering in the West Antarctic peninsula indicate that the rate of chemical weathering per unit area in these regions could be significant compared to temperate regions (Lyons et al., 2015). Recently, Torres, Moosdorf, Hartmann, Adkins, and West, (2017) have demonstrated based on the global compilation of hydro-chemical data that weathering fluxes yield from the glacierized catchments are higher than the global average and therefore highlighted dominant role of glacial weathering. However, in this compilation, most of the

Accepted Article

This article is protected by copyright. All rights reserved.

hydro-chemical data of the glacierized catchments are only available from the tropical and subtropical regions. Therefore, considering the vast glacierized area of Antarctica and absence of any anthropogenic activities, this region provides us a unique opportunity to understand glacial mediated chemical weathering in a pristine environment.

The objectives of the present study are to investigate lake water chemistry and chemical weathering processes in the Larsemann Hills region, East Antarctica during austral summer. Based on chemical (dissolved major ions, Sr and $^{87}Sr/^{86}Sr$) datasets and their inverse modelling, we have apportioned solute sources and quantified their contributions to chemical budgets of these lake waters. Finally, these results have led us to estimate silicate weathering rates (SWR) and their corresponding atmospheric CO_2 consumptions in the catchments of the East Antarctic lakes. We have also investigated primary controlling factors of chemical weathering processes in the Larsemann Hills, East Antarctica.

2. Study Area

The present study focuses on chemical and Sr isotopic characterizations of ten lakes from the coastal regions of the Prydz Bay (69°20'S-69°34'S, 66°E-79°E), East Antarctica (Figure 1). The Bay is located near the Princess Elizabeth land and is surrounded by more than a hundred ice-free islands, covering an area of ~100 km^2. These areas have been sub-grouped into three regions, namely Larsemann Hills (LH), Rauer Group and Vestfold Hills. The main water sources for the Bay are the meltwater from the Amery ice shelf and neighbouring ice sheets (Hodgson et al., 2016). The lakes investigated in the present study are from the Larsemann Hills, which is extended over an area of ~50 km^2 (Figure 1). The basement rock of the LH comprises of layered complex of iron-rich gneiss and heterogeneous garnet-bearing

Accepted Article

This article is protected by copyright. All rights reserved.

migmatitic paragneiss of Meso- to Neo-Proterozoic age. Besides, occurrence of sillimanite, spinel, cordierite, garnet, K-feldspar, biotite and intrusion of metapelites lenses have also been reported in these basement rocks (Carson, Dirks, Hand, Sims, & Wilson, 1995; Stüwe, Braun, & Peer, 1989). A thin layer of permafrost occur seasonally at a water depth of 0.3-0.9 m (Kaup & Burgess, 2002; Shevnina & Kourzeneva, 2017). A previous study based on elemental compositions of the topsoil in the Larsemann Hills found compositionally immature, which hints at slow but active on-going weathering in this region (Shi, Teng, Ma, Wang, & Li, 2018).

2.1. Geohydrology and Climate

More than 150 freshwater lakes, ranging from small to deep glacial water bodies, are present in the Larsemann Hills (Liu et al., 2007). These lakes, owing to low nutrient availability and biological productivity, are generally oligotrophic in nature (Sabbe et al., 2003). Although the origin of these lakes has not been well understood, isostatic readjustment due to multiple advancement and retreat of glaciers may have played a key role in the formation process (Burton, 1981; Hodgson et al., 2005). These water bodies are mainly fed by meltwater supplies during austral summer (December, January, and February) through small streams and channels. Available limited discharge data for selected lakes from this region indicates that the daily water flow varies between 0.02 and 1.6 m^3/s (Shevnina & Kourzeneva, 2017). The amount of water available in the stream is meagre during austral winter and mainly comes from basal melting of snow/ice sheet. The monthly mean temperatures in these regions fluctuate significantly during summer (~0°C) and winter (-18 to -15 °C) seasons (Gillieson, Burgess, Spate, & Cochrane, 1990). In addition to these climatic

Accepted Article

This article is protected by copyright. All rights reserved.

variations, strong katabatic westerlies leave imprints of wind erosion (e.g. honeycomb structures) onto the North-South facing hillocks (Spate, Burgess, & Shevlin, 1995). The strong winds cause internal mixing in ice-free lakes whereas perennially ice-covered lakes are less affected. Small physical and chemical stratifications are found in these ice-covered lakes. Earlier studies have confirmed the minimal anthropogenic impact on the water chemistry of these lakes (Gasparon & Matschullat, 2006a, 2006b; Kaup & Burgess, 2002).

2.2. Analytical Methodology

Twenty-eight surface and bottom water samples from ten LH lakes were collected during the austral summer of 2017 (Figure 1). About 2 litres of these samples were collected using Niskin bottles from a coring platform attached with metal-free rubber pontoon. The depths corresponding to benthic samples were measured manually using a graduated pole. The pH and temperature of the samples were measured on-site using a portable sensor. Samples were collected in pre-cleaned HDPE bottles. These bottles were rinsed with ambient water before sample collection. We have filtered these samples using 0.45 μm cellulose acetate filters within 24 hrs of their collection. The filtered samples were split into two aliquots and one of these aliquots was acidified with ultra-pure HNO_3 acid to pH~2.

Alkalinities of the samples were measured in their unacidified aliquot using the Gran-titration method adopted from Tripathy, Mishra, Danish and Ram (2019). Selected nutrients (silicates and nitrates) were measured in the unacidified aliquot (stored at -20°C until analyses) using an automated-spectrophotometer. Major cations (Na^+, K^+, Ca^{2+}, Mg^{2+}) and anions (Cl^- and SO_4^{2-}) in the unacidified aliquot were measured using an Ion chromatograph

Accepted Article

This article is protected by copyright. All rights reserved.

(Dionex) instrument. The water samples were passed through the IonPac CS17 column to separate cations and IonPac AS11-HC column to separate anions. The individual cation and anion peaks were quantified following a standard calibration approach to estimate the ionic concentrations. Reference standard solution (SLRS-6) was measured repeatedly to check accuracy of the measurements, whereas several replicates were analysed to constrain the analytical precision. The accuracy and precision of the measurements were better than 5%. Dissolved Sr concentrations were measured in acidified aliquots using a Quadrupole ICPMS (Agilent 7700x) instrument. Towards this, the signal of the ^{88}Sr isotope of the sample was quantified by a standard calibration approach. Freshwater reference standard SLRS-6 was measured at certain interval during the course of analysis. The measured Sr concentrations of the SLRS-6 (39.5 ng/g, n =5) were found consistent with its reported value (40.7 ± 0.3 ng/g). Replicate analyses of samples (n = 3) yielded a precision better than 3% for the Sr concentration measurements.

Sr isotopes were analysed in the filtered and acidified water samples using the multi-collector ICPMS (Neptune Plus, Thermo® Scientific) facility at NCPOR, Goa, India. These analyses were performed following the established analytical protocol of Rahaman and Singh (2012). Briefly, about 10 ml of water samples were passed through Eichrom Sr specific resin to extract pure Sr from the samples. This pure Sr aliquot was analysed for their isotopic compositions. The measured ^{86}Sr/^{88}Sr ratio was normalized to its natural value (0.1194) to correct for instrumental mass bias. A standard solution of NIST NBS-987 was measured at regular intervals during the course of analysis. Average ^{87}Sr/^{86}Sr value of NBS-987 during the period of this study yielded a value of 0.710280 ± 0.000011 (2σ, n = 5) and long-term

Accepted Article

This article is protected by copyright. All rights reserved.

value 0.71028 ± 10 ppm (2σ, n=363) (Anand et al., 2019) which are well within its recommended value (0.710250 ± 0.00040 (2 σ)). The Sr isotopic data are reported hereafter sample-standard bracketing normalization following the approach of Weis et al. (2006). Average total procedural blank for Sr isotopic measurement was ~150 pg which corresponds 0.02% of total Sr typically analysed in the samples and hence, no blank correction was done.

3. Results

Major ions, Sr concentration and its isotopic ratio for ten lakes from the Larsermann Hills, East Antarctica are provided in Table 1. The pH of these samples vary between 6.3 and 8.9 (mean: 7.3 ± 0.8; n = 24). Water samples from eight (out of ten) lakes exhibit strong pH-alkalinity co-variation ($r = 0.95$; $p < 0.01$; $n = 19$). The other two lakes (Fisher and L7 lakes) are characterized by significantly higher alkalinity (3989 ± 900 µM; 1σ) compared to that of the eight lakes (684 ± 548 µM; 1σ). Water temperatures of all samples range from 2.6 to 9.0°C (average: 6 ± 3°C). These values broadly follow a bi-modal (~3°C and 8°C) variation with relatively higher temperatures observed for semi-enclosed lakes with limited oceanic connections (Figure 1). The average total dissolved solid (TDS) in these lakes with warmer water (250 mg/L) is higher than those with colder water conditions (50 mg/L). Chemistry of these lake waters is mostly Na-Cl type (Figure 2), indicating the dominance of solute inputs from oceanic sources. Dissolved Na, on average, accounts for about 70% of the total cationic (TZ^+) load, whereas Mg and Ca contribute about 18% and 11% of the TZ^+. The Na concentrations vary widely from 880 µM to 15643 µM, and the lower Na values were observed for lakes with relatively lower temperatures. The average Cl/Na ratio (1.06 ± 0.10) of these samples is marginally lower than that of the seawater (1.166; Drever (1997)). The

Accepted Article

This article is protected by copyright. All rights reserved.

median value of Mg (360 µM) for these lakes is significantly higher than the global average (123 µM; Meybeck (2005). In contrast, the median value of Ca for these lakes (281 µM) and global rivers (297 µM; Meybeck (2005)) are similar. The K content (29-562 µM; Table 1) in these lakes accounts for only ~2% of the total TZ^+. The dissolved Si for most of the lakes (9 out of 10; excluding L7) vary between 1.8 and 21.6 µM, with an average value of 10 ± 6 µM. This average Si value is lower by an order of magnitude compared to that of reported value for global rivers (145 µM; Meybeck (2005). The Si content of the L7 lake (122-123 µM; n = 2) is anomalously higher than that of other Antarctic lakes (10 ± 6 µM; Table 1). Among the anions, dissolved Cl^- ion accounts for about 70% of the total anionic load (TZ^-). Alkalinity and sulphate in these lakes, on an average contribute, 21% and 8% of the TZ^-. The sulphate concentrations of theses lakes vary from 44 to 1046 µM. It is worth mentioning here that the highest sulphate concentration is observed for the Lake L7, for which the anomalously higher Si concentration was also observed. The average $SO_4/(SO_4+HCO_3)$ ratio, a possible tracer for carbonic versus sulphuric acid-mediated weathering intensity, for these lakes (excluding two outliers with extremely higher values (~0.7) from Unnamed lake) is found to be 0.15 ± 0.09. Despite large spatial variability in lake chemistry, most of the chemical constituents (*e.g.* Na, Mg, Cl, SO_4, Si and TDS) show minimal (less than 10%) depth variability in these lakes. In contrast, dissolved Ca and HCO_3 show (on an average) about 20% depth variability with relatively higher concentrations in the surface (than deep) water samples. Further, contrary to its general trend of insignificant variability, the sulphate concentrations in one of the (Progress Lake) lakes show about 40% change within a depth of 20 m (Table 1).

Accepted Article

This article is protected by copyright. All rights reserved.

The dissolved Sr concentrations of these lakes vary between 91 and 2832 nM, with a median value of 503 nM. This median value is significantly lower than that of reported for seawater (89 µM) and global rivers (1.27 µM; Peucker-Ehrenbrink, Miller, Arsouze, & Jeandel (2010). The average Sr concentration is the lowest for the Discussion Lake, whereas it is highest for the Fisher Lake (Figure 1). Despite of its large variability, the Sr concentrations show strong co-variation with their corresponding Ca ($r = 0.87$; $p < 0.01$; $n = 24$) and alkalinity ($r = 0.83$; $p < 0.01$; $n = 24$) values. Excluding L7 Lake, the Sr concentrations show no major change (within 10%) with water depths in these lakes. The $^{87}Sr/^{86}Sr$ ratios for the lake samples vary between 0.71105 and 0.72111, with an average of 0.715 ± 0.003. The average $^{87}Sr/^{86}Sr$ is found to be the highest for the Unnamed Lake, whereas it is lowest for the Merkwater Lake. These isotopic values are intermediate to that of the seawater (0.7092; Veizer (1989) and regional lithology (0.76; Sheraton, Black, & McCulloch (1984)). We observed that the Sr isotope profiles do not show depth variations and therefore suggest Sr isotope behave conservatively in these lake systems (Table 1).

4. Discussion

Chemical and Sr isotopic compositions of the LH lake waters are mostly regulated by the relative contribution from its major solute sources, which include seawater, precipitated snow/glacial meltwaters and chemical weathering of bed-rocks present in the basin (Angino & Armitage, 1963). The major rock-types observed in this basin are granitic/gneissic in nature (Figure 1). There have been no reports of carbonate exposure in this region. However, the presence of trace amounts of carbonates, owing to their faster dissolution kinetics, can influence the surface water chemistry significantly even in crystalline terrains (Jacobson &

Accepted Article

This article is protected by copyright. All rights reserved.

Blum, 2000; Lyons et al., 2005; Lyons et al., 2003). Average elemental ratios for these major sources are compiled from available literature and provided in Table 2. In addition to these major sources, freezing of seawater in polar regions may precipitate mirabilite (Na_2SO_4), hydrohalites (NaCl, $2H_2O$) and Ca-Mg rich salts (Bein & Arad, 1992; Lyons et al., 2017; Wilson, 1979). Dissolution of these minerals may also supply solutes to these lakes.

4.1. Possible solute sources for major ions

Ternary diagram of chemical datasets can provide qualitative information about possible sources and their relative contribution to the LH lakes. Figure 2 depicts the ternary plot for major cations and anions for these lakes. These data are mostly Na-Cl type, and distinctly different compared to that observed for the global average composition of rivers (Figure 2). In contrast, the lake data fall closer to the seawater end-member value, indicating the dominance of oceanic input of solutes to these aquatic systems. This observation is consistent with the trends of both the cations and anions (Figure 2). To better constrain these sources, we have evaluated the co-variation of dissolved chloride with key ionic species (*e.g.* Ca, Mg, alkalinity, and sulphates; Figure 3). The dissolved chloride ion is mostly supplied through oceanic sources and is almost absent in major rocks present in the catchments. This makes Cl^- ion a reliable tracer to assess seawater influence on lake water chemistry. Figure 3 indicates that the Ca, Mg and HCO_3 data fall above the average seawater values. This observed enrichment in these elements is attributable to their appreciable supply from the chemical weathering of bedrocks. However, the degree of enrichment due to chemical weathering input is observed to be different for these elements. The enrichment is found to be more prominent in the case of dissolved Ca (than Mg). The non-oceanic sources that can

Accepted Article

This article is protected by copyright. All rights reserved.

supply Ca are weathering of silicate and carbonate rocks and/or supply from Ca-Mg salts. In contrast to this, most of the dissolved sulphate data fall on the seawater line (Figure 3), indicating dominant contribution of seawater input for sulphate ion. This observation further ascertains the minimal impact of sulphide oxidation in supplying dissolved sulphate to these lakes. However, two data from the unnamed lake fall above the seawater line (Figure 3). These data hint at the additional supply of sulphate, possibly from the dissolution of Gypsum and/or sulphide oxidation. As there have been no gypsum exposures in the basin, we attributed these enriched sulphate values of the unnamed lake to oxidation of sulphides. In contrast, a few SO_4 data also (from Fisher and Reid lakes) fall below the seawater. This lower dissolved sulphate concentration compared to seawater has been interpreted as removal of SO_4 through Na_2SO_4 precipitation during the freezing of seawater (Dickson, Head, Levy, & Marchant, 2013; Herut, Starinski, Katz, & Bein, 1990).

Like for any chemical constituent, the dissolved (Ca+Mg) concentrations of these LH lakes are likely to be supplied through oceanic sources and/or weathering processes (Lyons et al., 2017). To better constrain the weathering process, we estimated the non-sea-salt component of all the elements using the following equation

$$X_{NSS} = X_{lake} - (Cl_{lake} \times (X/Cl)_{SW}) \qquad (1)$$

where, the subscripts *lake*, *SW* and *NSS* stand for the measured lake water composition, seawater composition and non-seasalt component of the element, X (= Na, K, Ca, Mg, SO_4, HCO_3 and Sr) respectively. The average non-seasalt components for Ca and Mg in these lakes are found to be 71 ± 13% and 20 ± 14%, respectively. These components are lower

Accepted Article

This article is protected by copyright. All rights reserved.

compared to that computed for the alkalinity (98 ± 1%), which is predominantly supplied through non-oceanic sources. Dissolved alkalinity in aquatic systems is mostly supplied through CO_2-mediated weathering processes and these land-surface processes supply (Ca+Mg) and alkalinity in a fixed proportion of 2:1 ratio (in molar units; (Jacobson, Blum, & Lynn, 2002). We have compared the seawater-corrected (Ca+Mg) and alkalinity (in Eq units) for the lakes investigated in the present study (Figure 4). Most of the lake samples fall below the 1:1 line and the average (Ca+Mg)/alkalinity ratio for these samples is found to be ~0.78 which is lower than the expected value of 1.0. The exact cause for this depleted ratio is not known; we, however, hypothesize that the estimation of the non-oceanic component by assuming all dissolved chloride from seawater sources may not be strictly valid. The computation of X_{NSS} with the assumption of all dissolved Cl is, therefore, underestimate the non-oceanic sources. A large number of studies have reported the supply of dissolved Ca and Cl ions from the dissolution of Ca-Mg rich salts (Dickson et al., 2013; Lyons et al., 2017; Wilson, 1979) to the Antarctic lakes. It is, therefore, likely that the LH lakes also receive an appreciable amount of Ca, Mg and Cl from these salts, produced during freezing-thawing of the seawater. This proposition is also consistent with the higher $(Ca+Mg)_{NSS}/Alkalinity_{NSS}$ ratios (3.5 to 3.8) observed for the unnamed lake (Figure 4). This observed excess (Ca+Mg) cannot also be attributed to dissolved sulphate ion and hence, need to be accounted for chloride-rich sources, such as $CaCl_2$ or $MgCl_2$ salt/brines. Consistent with this proposition, the impact of calcium-rich salts on water chemistry has already been reported for various Antarctica lakes, groundwater and subsurface waters (Toner & Sletten, 2013; Toner, Catling & Sletten, 2017). The occurrence of these $CaCl_2$ salts in these watersheds is primarily linked

Accepted Article

This article is protected by copyright. All rights reserved.

to cation exchange processes during the downward transport of Na-Cl rich brines (Toner & Sletten, 2013).

4.2. Sources for dissolved Sr and $^{87}Sr/^{86}Sr$

Dissolved Sr and $^{87}Sr/^{86}Sr$ found frequent applications in constraining sources and weathering pattern of watersheds (Bickle et al., 2005; Dalai, Krishnaswami, & Sarin, 2002; Galy & France-Lanord, 1999; Palmer & Edmond, 1992; Rai, Singh, & Krishnaswami, 2010; Tripathy, Singh, & Krishnaswami, 2012). The Sr isotopic compositions of major rock-types, such as silicates and carbonates, are characterized with distinct isotopic values and hence, serve as a reliable proxy to apportion their contribution. We have used $^{87}Sr/^{86}Sr$ ratio to infer about its possible sources and their relative contributions. Figure 5 depicts a mixing plot between Sr/Ca and $^{87}Sr/^{86}Sr$ ratios for the LH lakes. This plot also includes source compositions and their mixing trends. It may be noted that the Sr isotopic ratios are distinctly higher for the silicates compared to those for seawater and carbonates (or, Ca-rich minerals). The LH lake samples fall closer to the seawater end-member, confirming the dominance of the oceanic sources in supplying Sr to these lakes. In addition to seawater, the dataset fall closer to the seawater-carbonate mixing trend, suggesting an appreciable supply of Sr from these minerals with faster dissolution kinetics. The data, however, fall far from the silicate end-member indicating minimal Sr contributions from silicate weathering to the lake.

Seabirds and penguins excreta have also been invoked as a possible source to the chemistry of Antarctic lake water (Spurr, 1975). Further, the significance of this source in regulating the sedimentary Sr isotopic data was established by Liu et al. (2007) through investigation of $^{87}Sr/^{86}Sr$ data for lacustrine sediments and seabird excreta. These excreta are

Accepted Article

This article is protected by copyright. All rights reserved.

often enriched in P, C and N and may supply about 2.5 wt% of the animal body part per day (Scherer, Gibbons, Stoops, & Muller, 1995). Efforts are made in this study based on the distribution of PO_4 and PO_4-$^{87}Sr/^{86}Sr$ variation to assess the importance of this solute source to the dissolved Sr isotopic budget. The dissolved phosphate in these samples is (6.7 ± 2.1 µg/L; Table 1) lower than that of the earlier reported values for the glacial waters influenced by seabird excreta (~35 µg/L; Scherer et al. (1995)). Further, the phosphate shows no systematic trend with Sr. Based on these observations, we infer that the minimal impact of excreta supply to the dissolved Sr budget of these lakes in East Antarctica.

4.3. Source-apportionment modelling

We have used an inverse model involving mass balance calculations of chemical and Sr isotopic datasets to apportion solute sources for the LH lakes. The inversion approach has been successfully used to quantify source contribution to rivers and estimating erosion rates for these basins (Millot, Gaillardet, Dupré, & Allègre, 2003; Moon, Huh, Qin, & van Pho, 2007; Negrel, Allegre, Dupr, & Lewin, 1993; Tripathy & Singh, 2010; Wu, Huh, Qin, Du, & van Der Lee, 2005). Unlike rivers, the lake water chemistry is linked to various complex processes, which includes the intensity of chemical weathering, hydrological (evaporation and condensation) changes, biological activities, residence time of lake water and chemical constituents. The residence time of subglacial lake water from Eastern Antarctica have reported varying between 5000 and 125000 years (Kapitsa, Ridley, & de Q. Robin, 1996; Jean-Baptiste, Petit, & Lipenkov, 2001). Therefore, estimating erosion rates for the drainage basin of a lake system using a chemical mass balance approach is not straightforward. Although we recognize the limitation of this approach, attempts were made to estimate

Accepted Article

This article is protected by copyright. All rights reserved.

erosion rate in the lake catchments of LH, for which no literature data exists. The present approach based on the inverse model assumes that the LH lakes are in steady-state and all the chemical species used in the calculation have similar residence time for these lakes. Further, it was assumed that the biological activities in the LH lakes only influence the dissolved silica content of the lake and its impact is minimal for major ions and Sr concentrations. Based on these assumptions, this approach is expected to yield first-order chemical erosion rates averaged over the residence time of the elements.

Details on the method and the computational code adopted in this study are provided in Tripathy and Das (2014). Briefly, this method relies on a set of chemical mass balance equations which relates the measured data (lake water) and model (possible sources and their relative fractions) parameters:

$$\left(\frac{X}{Na}\right)_{lake} = \sum_{i}^{4}\left(\frac{X}{Na}\right)_{i} \times f_i(Na) \qquad (2)$$

$$\left[\frac{^{87}Sr}{^{86}Sr} \times \left\{\frac{Sr}{Na}\right\}\right]_{lake} = \sum_{i=1}^{4}\left(\frac{^{87}Sr}{^{86}Sr}\right)_{i} \times \left(\frac{Sr}{Na}\right)_{i} \times f_i(Na) \qquad (3)$$

$$1 = \sum_{i=1}^{4} \mathrm{f}_i(\mathrm{Na}) \qquad (4)$$

where, the subscript, *lake* stands for lake water composition whereas *i* (= 1, 2, 3, 4) stands for the four major solutes sources, which are seawater, snow, silicates and Ca-rich minerals (e.g. carbonates and Ca-Mg salts). The $f_i(Na)$ represents the fraction of dissolved Na derived from the source *i*. The model uses a non-linear Quasi-Newton optimization algorithm (Tarantola (2005)) to find the best fit between the observed data and model parameters. This iterative algorithm starts from a set of *a-priori* information for the model parameters and finds the best

Accepted Article

This article is protected by copyright. All rights reserved.

possible *a-posteriori* results which explain the Eq. (2-4) with the least residual. *A-priori* values (and associated uncertainties) for the Na-normalized ratios and $^{87}Sr/^{86}Sr$ for the end-member were compiled from the literature and are listed in Table 2. Average silicate composition has been ascertained using the bedrock data reported earlier for the Larsmann Hills (Sheraton et al., 1984; Stüwe et al., 1989). Besides, the leaching of aerosols can also be a source of solutes to these lakes. Earlier studies have shown that these sources mostly supply solutes similar to carbonate weathering (Lyons et al., 2017) and hence, are considered to be part of the "*Ca-rich mineral*" end-member.

Results from the inverse model on dissolved cations and Sr supplied from major sources are provided in Supplementary Table S1 (cf. Supplementary material). Two samples, one from L67 and Reid Lake, show anomalous results and hence, are not included in constraining the general trend of Antarctic lake chemistry. The anomalous samples from L67 are characterized with relatively higher Ca, Cl and Na compared to the other two samples from the lake, whereas the Reid lake sample has significantly lower Sr content with no change in $^{87}Sr/^{86}Sr$ when compared to other samples (Table 1). The dissolved cations of these lakes (Figure 6) is dominantly supplied by seawater (63 ± 15%), with additional contributions from snow (15 ± 7%), silicates (13 ± 8%) and Ca-rich minerals (9 ± 5%). In the case of dissolved Sr, these lakes mainly receive Sr through oceanic sources (91 ± 4%) with minor contributions from silicate/Ca-rich minerals (10 ± 4%). These results are consistent with our earlier discussions based on chemical and isotopic data distributions. The average silicate derived cations (Cat_s) for individual lakes vary between 8 and 24% (Figure 6). The higher

Accepted Article

This article is protected by copyright. All rights reserved.

Cat_s value is observed for the Fisher lake, with relatively warmer (~8.5°C) water column temperature. The lower Cat_s values are observed for Reid, Discussion and Scandrett lakes.

4.4. Silicate weathering rates and controlling factors

Efforts are made in this study to estimate the silicate weathering rates (SWR) and CO_2 consumption rates (CCR) for these basins from Eastern Antarctica. There has been very limited hydrological information on these lakes and hence, we recognize that the present estimates are likely to be associated with large uncertainties. The SWRs and CCRs have been calculated using the following equations (Dalai et al., 2002):

$$SWR = \frac{Q}{A} \times (Na_{Sil} + K_{Sil} + Ca_{Sil} + Mg_{Sil} + SiO_2) \qquad (5)$$

$$CCR = \frac{Q}{A} \times (Na_{Sil} + K_{Sil} + 2 \times (Ca_{Sil} + Mg_{Sil})) \qquad (6)$$

where Q is the water discharge to the lakes, whereas A stands for the drainage area for the watershed. The results obtained from the inverse model for silicate-derived Na, K, Ca and Mg are used in the equations (5-6) to estimate the erosion rates. The SWR estimated using equation 5 also accounts for the dissolved silica of the LH lake samples. We show in a subsequent discussion that a significant fraction of silica from the lake gets removed due to biological activities and hence, our SWR estimate is only a lower limit for the weathering intensity for silicates. Representative data on drainage area and water discharge is only available for the Scandrett lake (Shevnina & Kourzeneva, 2017) and hence, the weathering rate has been calculated for this lake system. Shevnina and Kourzeneva (2017) have reported water outflow (0.079 m^3/s) and creek catchment area (1.14 km^2) for this lake. Assuming a comparable amount of water flux into the lake and discharge for selected seasons (about three

Accepted Article

This article is protected by copyright. All rights reserved.

months), we have computed an annual water discharge of 5.4×10^8 L/yr for this lake. The estimated silicate weathering rates for the Scandrett lake basin is 3.6 ± 0.3 tons/km^2/yr, which corresponds to 1.4 ± 0.1 mm/yr. These weathering rates are lower than that reported for the average global river basins (Figure 7) (5.4 tons/km^2/yr (Gaillardet, Dupre, Louvat, & Alle`gre, 1999), Amazon (13.0 tons/km^2/yr), and Ganga (8.9 tons/km^2/yr; Krishnaswami and Singh (2005)). The estimated CO_2 consumption rates of the Scandrett lake basin (0.5 ± 0.2 × 10^5 moles/km^2/yr) is also found lower compared to that reported for the global average for rivers (0.9 × 10^5 moles/km^2/yr; Gaillardet et al., 1999). These lower weathering rates are consistent with the colder climatic regimes particularly in the polar conditions, which is less conducive for weathering of resistant silicate minerals.

In an interesting observation of the present study, the dissolved silica concentrations in these Antarctic lakes (range from 3 µM to 100 µM with an average 18.94 µM; Table 1) were found systematically lower by an order of magnitude than that of the average global rivers (Gaillardet et al., 1999). Dissolved silica in any aquatic basin is mainly derived from silicate weathering, however, later could be altered by biological activities. To better understand the silicon cycle, we estimated the CO_2 consumption rates independently by using Si concentration of the lakes and its behaviour during the alumino-silicate weathering process. Huh, Tsoi, Zaitsev, and Edmond (1998), based on global riverine datasets, have suggested that the amount of CO_2 consumed from basins is equal to twice the silica concentrations. This approach yields a CO_2 consumption rate of (0.02 ± 0.001) × 10^5 moles/km^2/yr. This rate is about 95% lower than that estimated using silicate-derived cations in the present study. The exact cause of this difference is unclear. A possible explanation is

Accepted Article

This article is protected by copyright. All rights reserved.

removal of dissolved silica through biological pathways to support lake productivity which is needed to be understood in more detail, however, it is beyond the scope in the present study. Recent study (Hawkings et al., 2017) has highlighted export of amorphous silica to ocean produced by the Greenland ice sheet during aqueous weathering processes such as dissolution-precipitation mechanism in sub glacial environments. Similar processes have already been invoked for large river systems. For instance, Fontorbe, De La Rocha, Chapman, and Bickle (2013), based on silicon isotopic investigations, have suggested about 50% removal of dissolved silica from the Gangetic plain. We suggest similar processes to explain about 95% lower silica content in the Scandrett Lake. This proposition, however, needs to be tested thoroughly and a systematic study of silicon isotopes in dissolved and its counter phase i.e. lake sediments of water-bodies from Antarctica.

5. Conclusions

In this contribution, we have investigated the chemical and Sr isotopes of ten coastal lakes from East Antarctica to decipher solute sources, and estimate the rate of glacial induced chemical weathering in their catchments. Our important findings and their implications are concluded below.

The $^{87}Sr/^{86}Sr$ of these lake waters is close to global seawater and Antarctica snows, indicating a dominant role of seawater and snow precipitation in regulating the solute chemistry. Results of inverse modelling show that the cations are dominantly supplied from oceanic sources (80 ± 5%), with a less but significant contributions from weathering of carbonates and silicates (together contributing 20 ± 10%). Computations of the results from the inverse model yielded SWR of 1.4 ± 0.1 mm/yr which is lower than the global average (2.08 mm/yr).

Accepted Article

This article is protected by copyright. All rights reserved.

Our estimate of SWR and corresponding CO_2 consumption rates are slightly lower (~0.6 times) that of the global average reported for the global river basins. Though chemical weathering is lower, but, considering vast regions of Antarctica that went through glacial waxing and waning in areal coverage; for example exposure of large ice-free regions during the last interglacial and mid-Pliocene warm periods. This could be a potential region for silicate weathering and atmospheric CO_2 consumptions, unaccounted so far in the global estimates and hence could be a source of uncertainty.

Anomalous removal of silica (~95%) produced during weathering, for which the reason is still unknown which could be the scope for future investigations.

Acknowledgement

We acknowledge Ministry of Earth Sciences, Director NCPOR for financial support, and UGC for fellowship support during the study. Authors thank Ms. Lathika N, members of the 36th Indian Antarctic expedition and Dr. NS Magesh for their help during analysis, sampling and map preparation respectively. We also thank Dr. David Boutt for editorial efforts, Dr. Michael Gooseff and one anonymous reviewer for constructive comment and suggestions. This is NCPOR contribution number J-51/2019-20.

Accepted Article

This article is protected by copyright. All rights reserved.

6. References

Anand, S.S., Rahaman, W., Lathika, N., Thamban, M., Patil, S., & Mohan, R. (2019). Trace elements and Sr, Nd isotope compositions of surface sediments in the Indian Ocean: An evaluation of sources and processes for sediment transport and dispersal. *Geochemistry, Geophysics, Geosystems*, *20*, 3090– 3112. doi: 10.1029/2019GC008332

Angino, E. E., & Armitage, K. B. (1963). A geochemical study of lakes Bonney and Vanda, Victoria land, Antarctica. *The Journal of Geology, 71*(01), 89-95.

Bein, A., & Arad, A. (1992). Formation of saline groundwaters in the Baltic region through freezing of seawater during glacial periods. *Journal of Hydrology*, *140*, 75-87.

Bickle, M. J., Chapman, H. J., Bunbury, J., Harris, N. B. W., Fairchild, I. J., Ahmad, T., & Pomiès, C. (2005). Relative contributions of silicate and carbonate rocks to riverine Sr fluxes in the headwaters of the Ganges. *Geochimica et Cosmochimica Acta*, *69*(9), 2221-2240. doi:10.1016/j.gca.2004.11.019

Blum, J. D., & Ere, Y. (1995). A silicate weathering mechanism linking increases in marine $^{87}Sr/^{86}Sr$ with global glaciation. *Nature, 373*, 415-418.

Burton, H. R. (1981). Chemistry, physics and evolution of Antarctic saline lakes. *Hydrobiologia*, *82*, 339-362.

Accepted Article

This article is protected by copyright. All rights reserved.

Campbell, I. B. & Claridge, G. G. C. (1987). Antarctica: Soils, Weathering Processes and Environment. *Amsterdam: Elsevier*.

Carpenter, J. H., & Manella, M. E. (1973). Magnesium to chlorinity ratios in seawater. *Journal of Geophysical Research, 78*(18), 3621-3626. doi:10.1029/JC078i018p03621

Carson, C., Dirks, P. H. G. M., Hand, M. P., Sims, J. P., & Wilson, C. J. L. (1995). Compressional and extensional tectonics in low-medium pressure granulites from the Larsemann Hills, East Antarctica. *Geological Magazine, 132*(2), 151-170.

Carson, C. J., & Grew, E. S. (2007). Geology of the Larsemann Hills, Antarctica First Edition (1:25000 scale map) *Geoscience Australia, Canberra*.

Culkin, F., & Cox, R. A. (1966). Sodium, potassium, magnesium, calcium and strontium in sea water. *Deep-Sea Research, 13*.

Cuozzo, N., Sletten, R.S., Hu, Y., Liu, L., Teng, F., & Hagedorn, B. (2019). Silicate weathering in antarctic ice-rich permafrost: Insights using magnesium isotopes, *Geochimica et Cosmochimica Acta, (in press)*. doi: 10.1016/j.gca.2019.07.031.

Dalai, T. K., Krishnaswami, S., & Sarin, M. M. (2002). Major ion chemistry in the headwaters of the Yamuna river system: Chemical weathering, its temperature dependence and CO_2 consumption in the Himalaya. *Geochimica et Cosmochimica Acta, 66*(19), 3397-3416.

Accepted Article

This article is protected by copyright. All rights reserved.

Delmonte, B., Baroni, C., Andersson, P. S., Narcisi, B., Salvatore, M. C., Petit, J. R., . . . Maggi, V. (2013). Modern and Holocene aeolian dust variability from Talos Dome (Northern Victoria Land) to the interior of the Antarctic ice sheet. *Quaternary Science Reviews, 64*, 76-89. doi:10.1016/j.quascirev.2012.11.033

Dickinson, W.W., & Rosen M.R. (2003). Antarctic permafrost: An analogue for water and diagenetic minerals on Mars. *Geology, 31*(3), 199-202

Dickson, J. L., Head, J. W., Levy, J. S., & Marchant, D. R. (2013). Don Juan Pond, Antarctica: near-surface $CaCl_2$-brine feeding Earth's most saline lake and implications for Mars. *Sci Rep, 3*, 1166. doi:10.1038/srep01166

Drever, J. I. (1997). The Geochemistry of Natural waters, 3rd edition. *Prentice Hall New Jersey*, 215-234.

Fontorbe, G., De La Rocha, C. L., Chapman, H. J., & Bickle, M. J. (2013). The silicon isotopic composition of the Ganges and its tributaries. *Earth and Planetary Science Letters, 381*, 21-30. doi:10.1016/j.epsl.2013.08.026

Foster, G. L., & Vance, D. (2006). Negligible glacial–interglacial variation in continental chemical weathering rates. *Nature, 444*(7121), 918-921. doi:10.1038/nature05365

Fretwell P., Pritchard H. D., Vaughan D.G., Bamber J.L., Barrand N.E., Bell R., . . . Zirizzotti A. (2013). Bedmap2:improved ice bed, surface and thickness datasets for Antarctica. *The Cryosphere* 7(1), 375-393. doi:10.5194/tc-7-375-2013

Accepted Article

This article is protected by copyright. All rights reserved.

Gaillardet, J., Dupre, B., Louvat, P., & Alle`gre, C. J. (1999). Global silicate weathering and CO_2 consumption rates deduced from the chemistry of large rivers. *Chemical Geology, 159*, 3–30.

Galy, A., & France-Lanord, C. (1999). Weathering processes in the Ganges–Brahmaputra basin and the riverine alkalinity budget. *Chemical Geology, 159*, 31-60.

Gasparon, M., & Matschullat, J. (2006a). Geogenic sources and sinks of trace metals in the Larsemann Hills, East Antarctica: Natural processes and human impact. *Applied Geochemistry, 21*(2), 318-334.

Gasparon, M., & Matschullat, J. (2006b). Trace metals in Antarctic ecosystems: Results from the Larsemann Hills, East Antarctica. *Applied Geochemistry, 21*(9), 1593-1612. doi:10.1016/j.apgeochem.2006.05.007

Gibbs, M. T., & Kump, L. R. (1994). Global chemical erosion during the Last Glacial Maximum and the present: Sensitivity to changes in lithology and hydrology. *Paleoceanography, 9*(4), 529-543. doi:10.1029/94pa01009

Gibson, E. K., Wentworth, S. J., & McKay, D. S. (1983), Chemical weathering and diagenesis of a cold desert soil from Wright Valley, Antarctica: An analog of Martian weathering processes. *J. Geophys. Res., 88*(02), 912– 928. doi:10.1029/JB088iS02p0A912.

Gillieson, D., Burgess, J. S., Spate, A., & Cochrane, A. (1990). An atlas of the lakes of the Larsemann Hills, Princess Elizabeth Land, Antarctica. *ANARE Research Notes No. 74*, 173 pp.

Accepted Article

This article is protected by copyright. All rights reserved.

Grew, E. S., Carson, C. J., Christy, A. G., & Boger, S. D. (2013). Boron- and phosphate-rich rocks in the Larsemann Hills, Prydz Bay, East Antarctica: tectonic implications. *Geological Society, London, Special Publications, 383*(1), 73-94. doi:10.1144/sp383.8

Grotti, M., Soggia, F., Ardini, F., Magi, E., Becagli, S., Traversi, R, & Udisti, R. (2015). Year-round record of dissolved and particulate metals in surface snow at Dome Concordia (East Antarctica). *Chemosphere, 138,* 916-923. doi:10.1016/j.chemosphere.2014.10.094

Hallet, B., Hunter, L., & Bogen, J. (1996). Rates of erosion and sediment evacuation by glaciers: A review of field data and their implications. *Global and Planetary Change, 12*, 213-235.

Hawkings J.R., Wadham J.L., Hendry K.R., Tranter M., Tedstone A., Nienow P., . . . Raiswell R. (2017). Ice sheets as a missing source to silica to the polar oceans. *Nature communications*, 8:14198. doi: 10.1038/ncomms14198

Heldmann, J.L., Pollard, W., McKay, C.P., Marinova, M.M., Davila, A., Williams, K.E., . . . Andersen, D.T. (2013). The high elevation Dry Valleys in Antarctica as analog sites for subsurface ice on Mars. *Planetary and Space Science, 85,* 53-58. doi:10.1016/j.pss.2013.05.019.

Herman, F., Seward, D., Valla, P. G., Carter, A., Kohn, B., Willett, S. D., & Ehlers, T. A. (2013). Worldwide acceleration of mountain erosion under a cooling climate. *Nature, 504*(7480), 423-426. doi:10.1038/nature12877

Accepted Article

This article is protected by copyright. All rights reserved.

Herut, B., Starinski, A., Katz, A., & Bein, A. (1990). The role of seawater freezing in the formation of subsurface brines. *Geochimica et Cosmochimica Acta, 54*, 13-21.

Hodgson D. A., Verleyen E., Sabbe K., Squier A. H., Keely B.J., Leng M. J., . . . Vyverman, W. (2005). Late Quaternary climate-driven environmental change in the Larsemann Hills, East Antarctica, multi-proxy evidence from a lake sediment core. *Quaternary Research, 64*, 83-99. doi:10.1016/j.yqres.2005.04.002

Hodgson, D. A., Noon, P. E., Vyverman, W., Bryant, C. L., Gore, D. B., Appleby P., . . . Wood, P.B. (2012). Were the Larsemann Hills ice-free through the Last Glacial Maximum?. *Antarctic Science, 13*(4), 440-454. doi:10.1017/S0954102001000608

Hodgson, D. A., Whitehouse, P. L., Gijs De Cort, Berg, S., Verleyen, E., Tavernier, I., Stephen R., . . . O' Brien, P. (2016). Rapid early Holocene sea-level rise in Prydz Bay, East Antarctica. *Global and Planetary Change, 139*, 128-140. doi:10.1016/j.gloplacha.2015.12.020

Huh, Y., Tsoi, M.-Y., Zaitsev, A., & Edmond, J. M. (1998). The fluvial geochemistry of the rivers of Eastern Siberia: I. Tributaries of the Lena River draining the sedimentary platform of the Siberian Craton. *Geochimica et Cosmochimica Acta, 62*(10), 1657-1676.

Jacobson, A. D., & Blum, J. D. (2000). Ca/Sr and $^{87}Sr/^{86}Sr$ geochemistry of disseminated calcite in Himalayan silicate rocks from Nanga Parbat:Influence on river-water

Accepted Article

This article is protected by copyright. All rights reserved.

chemistry. *Geology, 28*(5), 463. doi:10.1130/0091-7613(2000)28<463:sasgod>2.0.co;2

Jacobson, A. D., Blum, J. D., & Lynn, W. M. (2002). Reconciling the elemental and Sr isotope composition of Himalayan weathering fluxes: Insights from the carbonate geochemistry of stream waters. *Geochimica et Cosmochimica Acta, 66*(19), 3417-3429.

Jean-Baptiste, P., Petit, J., & Lipenkov, V. (2001). Constraints on hydrothermal processes and water exchange in Lake Vostok from helium isotopes. *Nature,* 411**,** 460–462 doi:10.1038/35078045

Kapitsa, A., Ridley, J., & de Q. Robin, G. (1996). A large deep freshwater lake beneath the ice of central East Antarctica. *Nature,* 381**,** 684–686 doi:10.1038/381684a0

Kaup, E. N. N., & Burgess, J. S. (2002). Surface and subsurface flows of nutrients in natural and human impacted lake catchments on Broknes, Larsemann Hills, Antarctica. *Antarctic Science, 14*(4), 343-352. doi:10.1017/s0954102002000123

Krishnaswami, S., & Singh, S. K. (2005). Chemical weathering in the river basins of the Himalaya, India. *Current Science, 89*(5), 10.

Liu, X., Sun, L., Xie, Z., Yin, X., Zhu, R., & Wang, Y. (2007). A preliminary record of the historical seabird population in the Larsemann Hills, East Antarctica, from geochemical analyses of Mochou Lake sediments. *Boreas, 36*(2), 182-197. doi:10.1080/03009480600991789

Accepted Article

This article is protected by copyright. All rights reserved.

Lyons, W. B., Bullen, T. D., & Welch, K. A. (2017). Ca isotopic geochemistry of an Antarctic aquatic system. *Geophys. Res. Lett.*, *44*, 882-891. doi:10.1002/2016GL071169.

Lyons, W. B., Dailey, K. R., Welch, K. A., Deuerling, K. M., Welch, S. A., & McKnight, D. M. (2015). Antarctic streams as a potential source of iron for the Southern Ocean. *Geology*, *43*(11), 1003-1006. doi:10.1130/g36989.1

Lyons, W. B., Dowling, C., Welch, K. A., Synder, G., Poreda, J. R., Doran, T.P., & Fountain, A. (2005). Dating water and solute additions to ice-covered Antarctic lakes *Goldschmidt Conference Abstracts 2005*, A720.

Lyons, W. B., Welch, K. A., Fountain, A. G., Dana, G. L., Vaughn, B. H., & McKnight, D. M. (2003). Surface glaciochemistry of Taylor Valley, southern Victoria Land, Antarctica and its relationship to stream chemistry. *Hydrological Processes*, *17*(1), 115-130. doi:10.1002/hyp.1205

Maas, R., Grew, E. S., & Carson, C. J. (2015). Isotopic constrain (Pb, Rb-Sr, Sm-Nd) on the sources of Early Cambrian pegmatites with Boron and Beryllium minerals in the Larsemann Hills, Prydz Bay, Antarctica. *The Canadian Mineralogist*, *53*(2), 249-272. doi:10.3749/canmin.1400081

Meybeck, M. (2005). Looking for water quality. *Hydrological Processes*, *19*(1), 331-338. doi:10.1002/hyp.5778

Accepted Article

This article is protected by copyright. All rights reserved.

Millot, R., Gaillardet, J. é., Dupré, B., & Allègre, C. J. (2003). Northern latitude chemical weathering rates: clues from the Mackenzie River Basin, Canada. *Geochimica et Cosmochimica Acta, 67*(7), 1305-1329. doi:10.1016/s0016-7037(02)01207-3

Moon, S., Huh, Y., Qin, J., & van Pho, N. (2007). Chemical weathering in the Hong (Red) River basin: Rates of silicate weathering and their controlling factors. *Geochimica et Cosmochimica Acta, 71*(6), 1411-1430. doi:10.1016/j.gca.2006.12.004

Morlighem, M., Rignot, E., Binder, T. Blankenship D., Drews R.,Eagles, G., ... Young D.A. (2019). Deep glacial troughs and stabilizing ridges unveiled beneath the margins of the Antarctic ice sheet. *Nature Geoscience* doi:10.1038/s41561-019-0510-8

Negrel, P., Allegre, C. J., Dupr, B., & Lewin, E. (1993). Erosion sources determined by inversion of major and trace element ratios and strontium isotopic ratios in river water: The Congo Basin case. *Earth and Planetary Science Letters, 120*, 59-76.

Nezat, C.A., Lyons, W.B., & Kathleen A. W. (2001) Chemical weathering in streams of a polar desert (Taylor Valley, Antarctica). *GSA Bulletin, 113(11)*, 1401–1408. doi:10.1130/0016-7606(2001)113<1401:CWISOA>2.0.CO;2

Palmer, M. R., & Edmond, J. M. (1992). Controls over the strontium isotope composition of river water. *Geochimica et Cosmochimica Acta, 56*, 2099-2111.

Peucker-Ehrenbrink, B., Miller, M. W., Arsouze, T., & Jeandel, C. (2010). Continental bedrock and riverine fluxes of strontium and neodymium isotopes to the oceans. *Geochemistry, Geophysics, Geosystems, 11*(3), doi:10.1029/2009gc002869

Accepted Article

This article is protected by copyright. All rights reserved.

Rahaman, W., & Singh, S. K. (2012). Sr and $^{87}Sr/^{86}Sr$ in estuaries of western India: Impact of submarine groundwater discharge. *Geochimica et Cosmochimica Acta, 85*, 275-288. doi:10.1016/j.gca.2012.02.025

Rai, S. K., Singh, S. K., & Krishnaswami, S. (2010). Chemical weathering in the plain and peninsular sub-basins of the Ganga: Impact on major ion chemistry and elemental fluxes. *Geochimica et Cosmochimica Acta, 74*(8), 2340-2355. doi:10.1016/j.gca.2010.01.008

Riebe, C. S., Kirchner, J. W., & Finkel, R. C. (2004). Erosional and climatic effects on long-term chemical weathering rates in granitic landscapes spanning diverse climate regimes. *Earth and Planetary Science Letters, 224*(3-4), 547-562. doi:10.1016/j.epsl.2004.05.019

Robert C., & Kennett J.P. (1997). Antarctic continental weathering changes during Eocene Oligocene cryosphere expansion: clay mineral and oxygen isotope evidence. *Geology, 25*, 587-590

Sabbe, K., Hodgson, D. A., Verleyen, E., Taton, A., Wilmotte, A., Vanhoutte, K., & Vyverman, W. (2004). Salinity, depth and the structure and composition of microbial mats in continental Antarctic lakes. *Freshwater Biology, 49*, 296-319.

Sabbe, K., Verleyen, E., Hodgson, D. A., Vanhoutte, K., & Vyverman, W. (2003). Benthic diatom flora of freshwater and saline lakes in the Larsemann Hills and Rauer Islands, East Antarctica. *Antarctic Science, 15*(2), 227-248. doi:10.1017/s095410200300124x

Accepted Article

This article is protected by copyright. All rights reserved.

Scherer, N. M., Gibbons, H. L., Stoops, K. B., & Muller, M. (1995). Phosphorus Loading of an Urban Lake by Bird Droppings. *Lake and Reservoir Management, 11*(4), 317-327. doi:10.1080/07438149509354213

Sheraton, J. W., Black, L. P., & McCulloch, M. T. (1984). Regional geochemical and isotopic characteristics of high-grade metamorphics of the Prydz bay area: The extent of proterozoic reworking of Qrchaean continental crust in East Antarctica. *Precambrian Research, 26*(2), 169-198. doi: 10.1016/0301-9268(84)90043-3

Shevnina, E., & Kourzeneva, E. (2017). Thermal regime and components of water balance of lakes in Antarctica at the Fildes peninsula and the Larsemann Hills. *Tellus A: Dynamic Meteorology and Oceanography, 69(1),* 1317202. doi:10.1080/16000870.2017.1317202

Shi, G., Teng, J., Ma, H., Wang, D., & Li, Y. (2018). Metals in topsoil in Larsemann Hills, an ice-free area in East Antarctica: Lithological and anthropogenic inputs. *Catena, 160,* 41-49. doi:10.1016/j.catena.2017.09.001

Singh, S. K., Sarin, M. M., & France-Lanord, C. (2005). Chemical erosion in the eastern Himalaya: Major ion composition of the Brahmaputra and $\delta^{13}C$ of dissolved inorganic carbon. *Geochimica et Cosmochimica Acta, 69*(14), 3573-3588. doi:10.1016/j.gca.2005.02.033

Accepted Article

This article is protected by copyright. All rights reserved.

Spate, A. P., Burgess, J. S., & Shevlin, J. (1995). Rates of rock surface lowering, Princess Elizabeth Land, Eastern Antarctica. *Earth Surface Processes and Landform*, *20*, 567-573.

Spurr, B. (1975). Limnology of Bird Pond, Ross Island, Antarctica. *New Zealand Journal of Marine and Freshwater Research*, *9*(4), 547-562. doi:10.1080/00288330.1975.9515588

Stüwe, K., Braun, H. M., & Peer, H. (1989). Geology and structure of the Larsemann Hills area, Prydz Bay, East Antarctica. *Australian Journal of Earth Sciences*, *36*(2), 219-241. doi:10.1080/08120098908729483

Tarantola, A. (2005). The least square criterion, in Inverse Problem theory and Methods for model parameter estimation *Soc. for Ind. and Appl. Math., Philadelphia, Pa*, 68-72.

Toner, J.D., & Sletten, R.S. (2013). The formation of Ca-Cl-rich groundwaters in the Dry Valleys of Antarctica: Field measurements and modeling of reactive transport, *Geochimica et Cosmochimica Acta*, *110*, 84-105. doi:10.1016/j.gca.2013.02.013.

Toner, J.D., Catling, D.C., & Sletten, R.S. (2017). The geochemistry of Don Juan Pond: Evidence for a deep groundwater flow system in Wright Valley, Antarctica. *Earth and Planetary Science Letters*, *474*, 190-197, doi:10.1016/j.epsl.2017.06.039.

Torres, M. A., Moosdorf, N., Hartmann, J., Adkins, J. F., & West, A. J. (2017). Glacial weathering, sulfide oxidation, and global carbon cycle feedbacks. *Proc Natl Acad Sci U S A*, *114*(33), 8716-8721. doi:10.1073/pnas.1702953114

Accepted Article

This article is protected by copyright. All rights reserved.

Tripathy, G. R., & Das, A. (2014). Modeling geochemical datasets for source apportionment: Comparison of least square regression and inversion approaches. *Journal of Geochemical Exploration, 144*, 144-153. doi:10.1016/j.gexplo.2014.03.004

Tripathy, G.R., Mishra, S., Danish, M., & Ram K. (2019). Elevated Barium concentrations in rain water from east-coast of India: role of regional lithology *Journal of Atmospheric Chemistry, 76(10)*, 59-72. doi:10.1007/s10874-019-9387-6

Tripathy, G. R., & Singh, S. K. (2010). Chemical erosion rates of river basins of the Ganga system in the Himalaya: Reanalysis based on inversion of dissolved major ions, Sr, and $^{87}Sr/^{86}Sr$. *Geochemistry, Geophysics, Geosystems, 11*(3). doi:10.1029/2009gc002862

Tripathy, G. R., Singh, S. K., & Krishnaswami, S. (2012). Sr and Nd Isotopes as Tracers of Chemical and Physical Erosion. *M. Baskaran (ed.), Handbook of Environmental Isotope Geochemistry, Advances in Isotope Geochemistry*. doi:10.1007/978-3-642-10637-8_26,#Springer-Verlag

Veizer, J. (1989). Strontium Isotopes in Sea Water Through Time. *Ann. Rev. Earth Planet. Sci, 17*, 141-167.

Velbel, M. A. (1993). Constancy of silicate-mineral weathering-rate ratios between natural and experimental weathering: implications for hydrologic control of differences in absolute rates. *Chemical Geology, 105*, 89-99.

Accepted Article

This article is protected by copyright. All rights reserved.

Verleyen, E., Hodgson, D. A., Sabbe, K., Cremer, H., Emslie, S. D., Gibson, J., . . . Vyverman, W. (2011). Post-glacial regional climate variability along the East Antarctic coastal margin—Evidence from shallow marine and coastal terrestrial records. *Earth-Science Reviews, 104*(4), 199-212. doi:10.1016/j.earscirev.2010.10.006

Weis, D., Kieffer, B., Maerschalk, C., Barling, J., de Jong, J., Williams, G. A., . . . Mahoney, J. B. (2006). High-precision isotopic characterization of USGS reference materials by TIMS and MC-ICP-MS. *Geochemistry, Geophysics, Geosystems, 7*(8). doi:10.1029/2006gc001283

West, A., Galy, A., & Bickle, M. (2005). Tectonic and climatic controls on silicate weathering. *Earth and Planetary Science Letters, 235*(1-2), 211-228. doi:10.1016/j.epsl.2005.03.020

White, A. F., & Blum, A. E. (1995). Effects of climate on chemical, weathering in watersheds. *Geochimica et Cosmochimica Acta, 59*(9), 1729-1747.

Wilson, A. T. (1979). Geochemical problems of Antractic dry areas. *Nature, 280*.

Wu, L., Huh, Y., Qin, J., Du, G., & van Der Lee, S. (2005). Chemical weathering in the Upper Huang He (Yellow River) draining the eastern Qinghai-Tibet Plateau. *Geochimica et Cosmochimica Acta, 69*(22), 5279-5294. doi:10.1016/j.gca.2005.07.001

Accepted Article

This article is protected by copyright. All rights reserved.

Zachos, J.C., Opdyke, B.N., Quinn, T.M., Jones, C.E. & Halliday, A.N. (1999). Early cenozoic glaciation, antarctic weathering, and seawater $^{87}Sr/^{86}Sr$: is there a link?. *Chemical Geology*, *161*(1–3), 165-180. doi: 10.1016/S0009-2541(99)00085-6.

Accepted Article

This article is protected by copyright. All rights reserved.

Accepted Article

Figure Captions

Figure 1: Location map of the ten coastal lakes near the Prydz Bay, East Antarctica. The regional geology of this region has also been shown (modified after Carson & Grew (2007)).

Figure 2: Ternary diagram for major cations and anions of the Antarctic lakes. For reference, average composition of possible major solute sources (seawater, Antarctica snow and silicate rocks) is also shown; See text for data source for the end-member compositions. The data distribution indicates dominancy of oceanic sources in regulating the lake water chemistry.

Figure 3: Co-variation of dissolved Mg, HCO_3, Ca and SO_4 with chloride ion. The straight line represents the average seawater composition. Enriched Ca and Mg with respect to the seawater line indicate their supply also from other sources, such as chemical weathering of bed-rocks and/or Ca-Mg rich salts.

Figure 4: Correlation plot between seawater-corrected alkalinity and (Ca+Mg) for the Antarctic lakes. The straight line represents the 1:1 line, a trend expected for chemical weathering of bedrocks.

Figure 5: Mixing diagram between Sr/Ca (molar ratio) and $^{87}Sr/^{86}Sr$ ratios of the Antarctic lakes. Chemical compositions for major solute sources (*cf.* text for data source) are also shown here. The data fall closer to the seawater end-member, hint at dominancy of oceanic solute supply to the lake.

Figure 6: Results from the inverse model on relative supply cations and strontium to the lakes from different sources.

This article is protected by copyright. All rights reserved.

Figure 7: Comparison of silicate weathering (tons/km^2/yr) and atmospheric CO_2 consumptions (10^5 mols/km^2/yr) rates of the Antarctic lake (this study) and global rivers.

Data availability statement

The data that support the findings of this study are openly available in the manuscript as Table 1, Table 2 and Supplementary Table S1.

Accepted Article

This article is protected by copyright. All rights reserved.

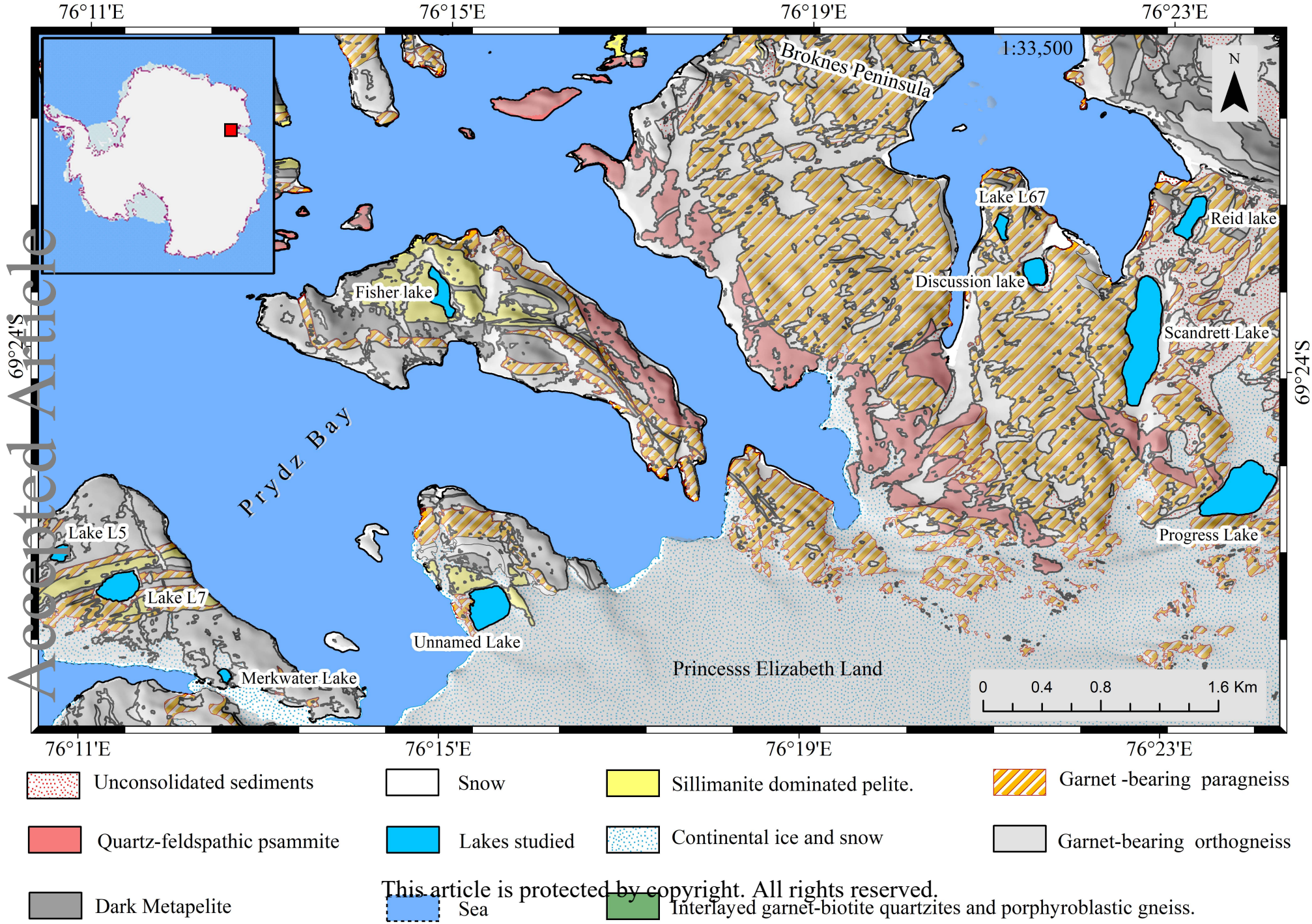

Accepted Article

This article is protected by copyright. All rights reserved.

Accepted Article

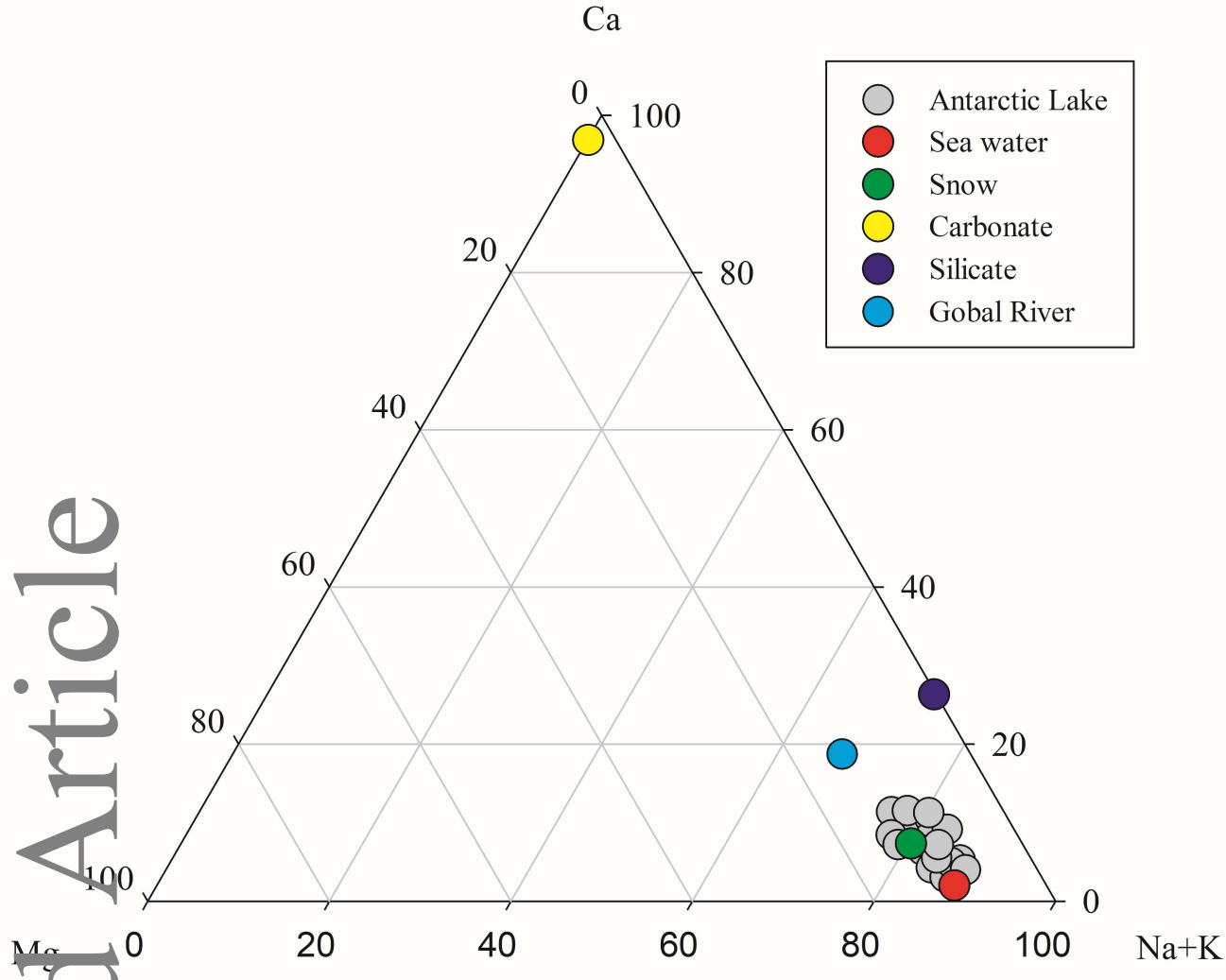

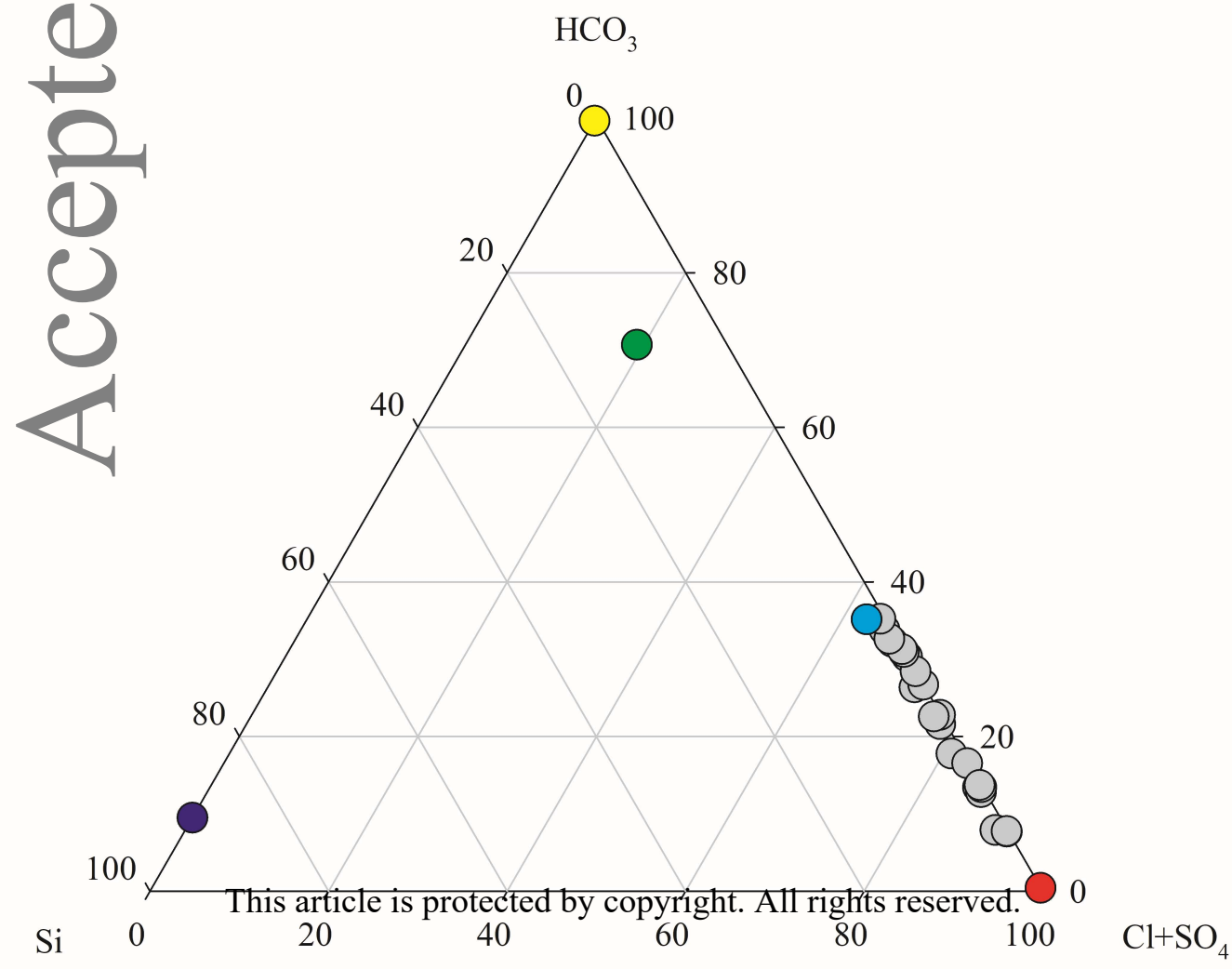

This article is protected by copyright. All rights reserved.

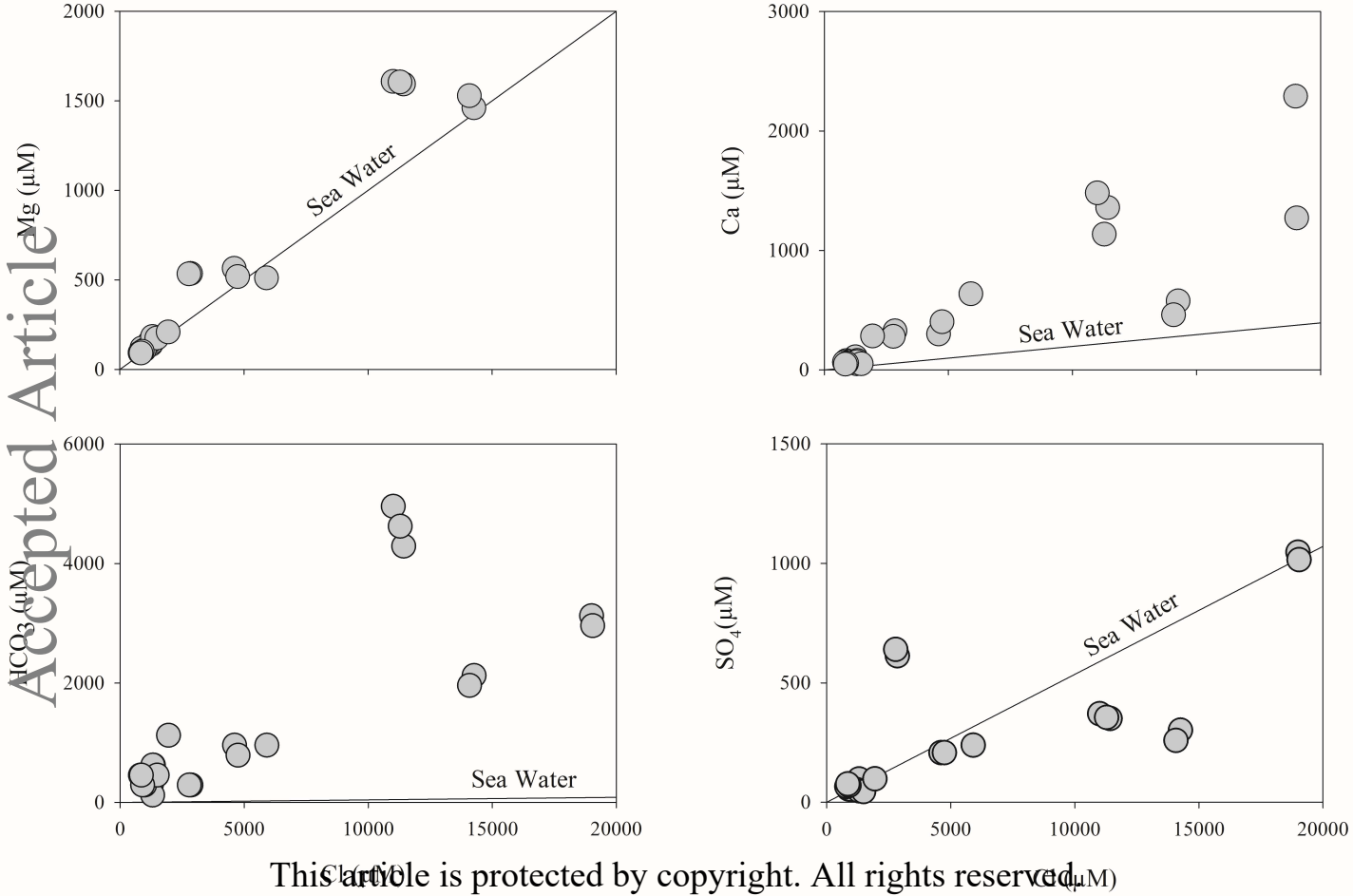

Accepted Article

This article is protected by copyright. All rights reserved.

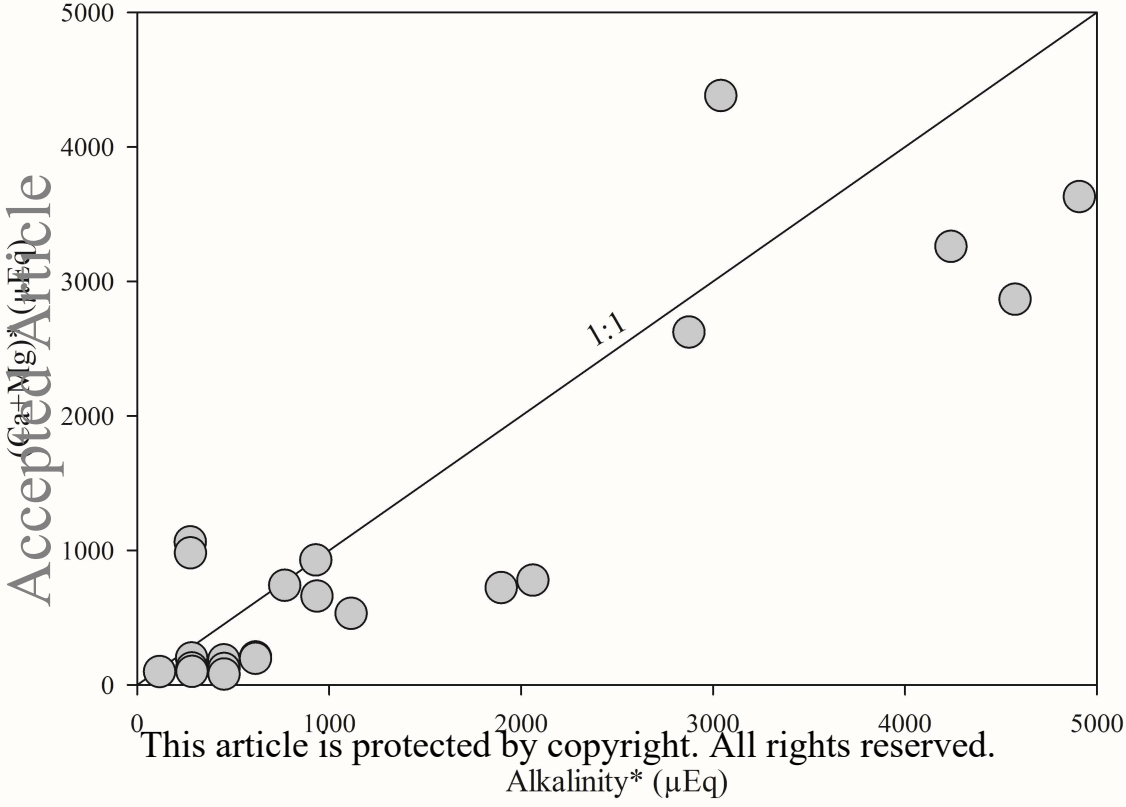

Accepted Article

This article is protected by copyright. All rights reserved.

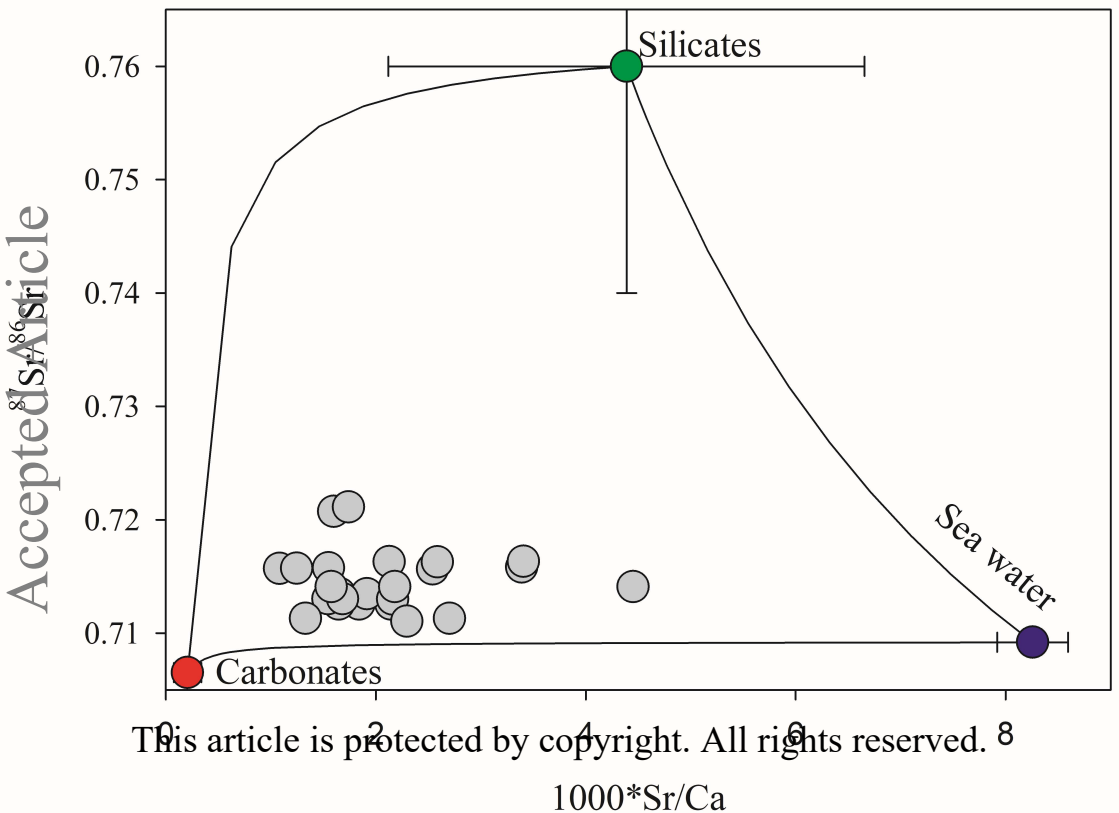

Accepted Article

This article is protected by copyright. All rights reserved.

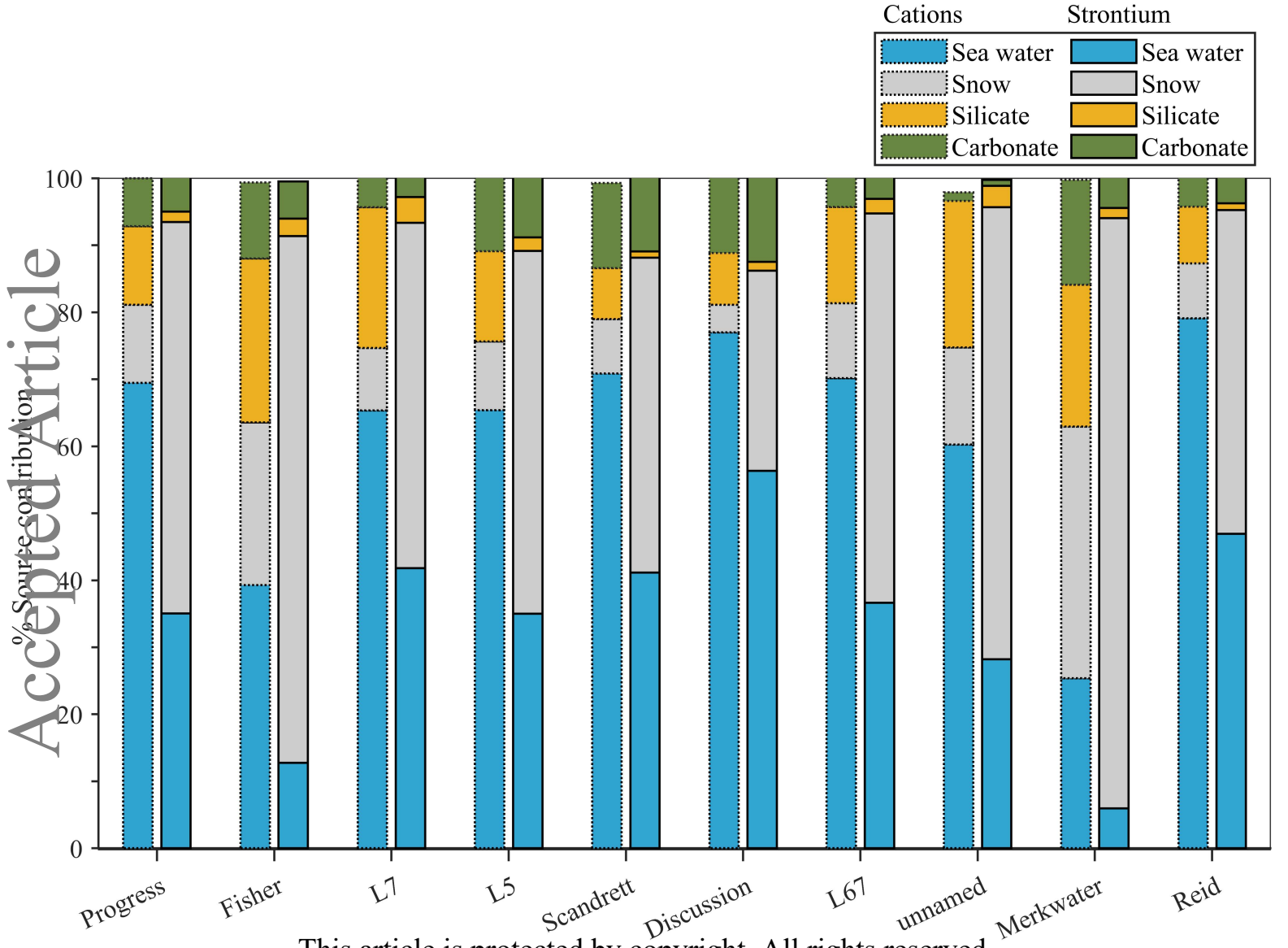

Accepted Article

This article is protected by copyright. All rights reserved.

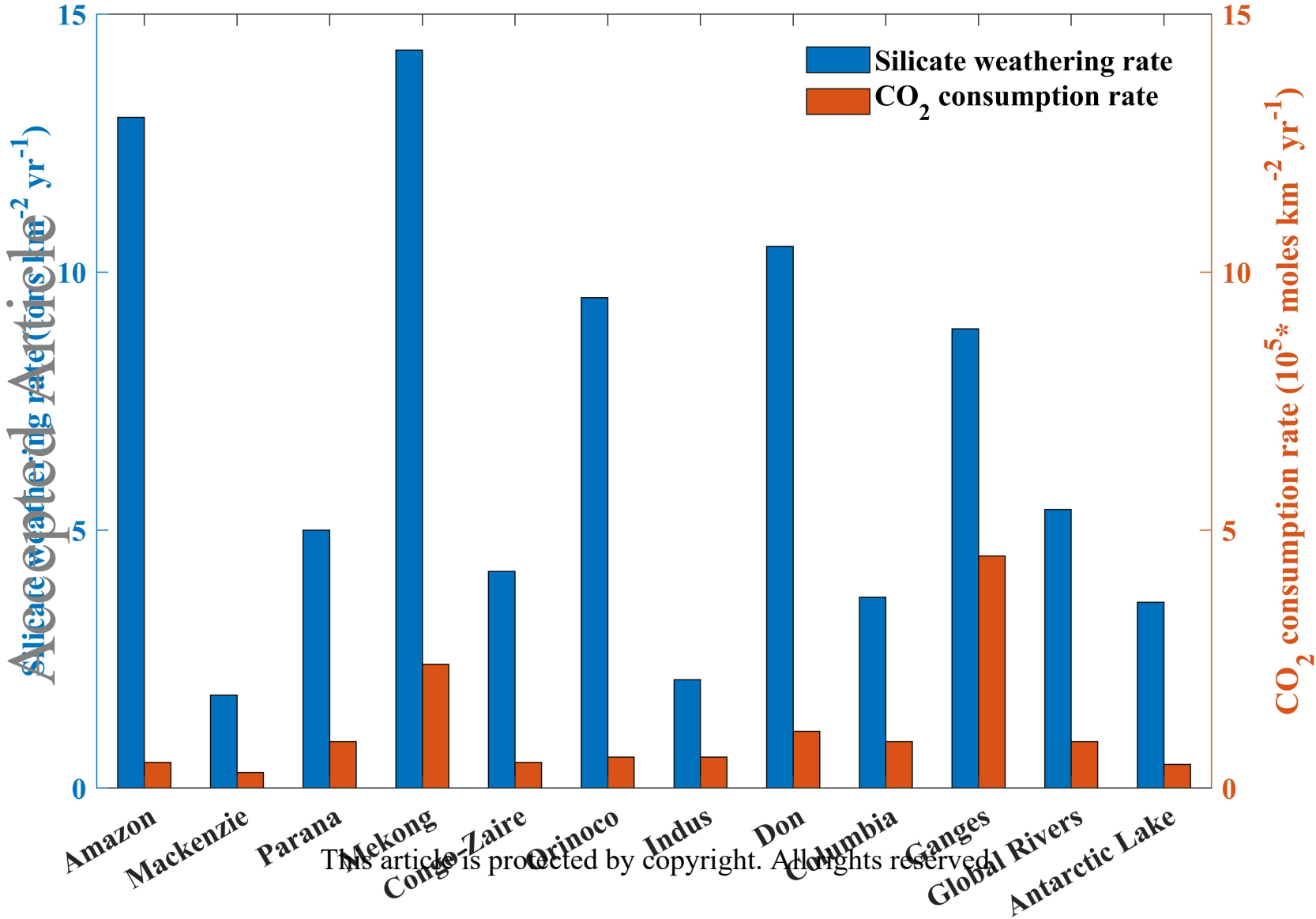

Accepted Article

This article is protected by copyright. All rights reserved.

Accepted Article

Table 1 Chemical and Sr isotopic data for the coastal lakes from the East Antarctica.

Lake (Lat.; Long.)	Sample ID	Depth (m)	pH	Temp. (ºC)	Na	K	Mg	Ca	Cl	HCO_3	SO_4	NO_3	Si	PO_4	TZ+	TZ-	NICB (%)	CSI	Sr (nM)	$^{87}Sr/^{86}Sr$
					μM															
Lake L7 (69° 24' 34.48"S 76° 11' 40.38"E)	L7_CS	Surface central	8.2	9.0	14938	562	2097	2290	19007	3122	1046	0.8	123	0.06	24274	24222	0.2	0.58	2483	0.71567
	L7_15	15	8.1	8.8	15643	509	2241	1271	19044	2956	1015	0.5	122	0.06	23176	24029	-3.6	0.21	1583	0.71568
Lake L67 (69° 23' 10.98"S 76° 20' 44.87"E)	L67_S1	Suface margin	7.1	8.7	5596	221	511	636	5915	956	238	0.1	11	0.07	8111	7347	9.9	-1.43	2832	0.71405
	L67_S2	surface central	7.2	8.7	4441	145	564	299	4613	956	207	0.1	11	0.09	6310	5982	5.3	-1.64	651	0.71405
	L67_C5	5	7.3	8.4	4485	170	517	401	4751	789	207	0.3	11	0.08	6492	5954	8.7	-1.50	632	0.71405
Fisher lake (69° 23' 28.26"S 76° 14' 58.28"E)	F_S2	Surface (margin)	8.5	8.7	10061	360	1594	1358	11431	4289	350	0.3	3	0.04	16323	16419	-0.6	0.83	2499	0.71251
	F_CS	Suface (central)	8.4	8.3	9748	179	1608	1480	11014	4956	370	0.3	3	0.05	16103	16710	-3.7	0.83	2437	0.71252
	F_10	10	8.4	8.5	9925	346	1605	1134	11292	4622	355	0.2	3	0.04	15748	16624	-5.4	0.69	2431	0.71251
Reid lake (69° 23' 08.83"S 76° 22' 42.36")	RL S	Surface central	8.8	8.1	12627	550	1461	577	14270	2122	301	0.2	6	0.08	17252	16994	1.5	0.43	1558	0.71126
	RL 3	3	8.9	8.1	13127	512	1528	460	14084	1956	258	0.1	6	0.06	17615	16556	6.2	0.39	612	0.71126
Unnamed lake (69° 24' 27.24"S 76° 15' 44.64"E)	BPL_S	Surface central	6.8	7.6	2901	97	535	325	2853	289	612	0.1	6	0.06	4717	4366	7.7	-2.54	519	0.72107
	BPL_3	3	6.8	7.6	2940	131	533	280	2792	289	639	0.3	6	0.10	4696	4360	7.4	-2.60	487	0.72068
Merd lake (69° 24' 53.43"S 76° 12' 46.66"E)	ML	Surface margin	8.0	6.4	1932	81	209	282	1950	1122	98	0.7	18	0.14	2994	3268	-8.7	-0.79	647	0.71101

This article is protected by copyright. All rights reserved.

Progress Lake (69° 24' 07.07"S; 76° 23' 17.85"E)	PG_S0	Surface central	6.4	4.4	1076	39	138	108	1264	289	53	0.3	22	0.05	1605	1659	-3.3	-3.38	167	0.71571
	PG_10	10	6.5	3.0	1161	44	150	49	1311	122	97	0.4	21	0.07	1605	1627	-1.4	-4.02	168	0.71577
	PG_25	20	6.3	2.7	1162	40	151	67	1203	456	52	0.4	21	0.09	1638	1763	-7.3	-3.52	170	0.71561
Nella Lake (69° 23' 35.44"S 76° 22' 17.12"E)	NL_S2	Surface (margin)	6.9	2.6	1315	60	181	77	1341	622	48	0.1	2	0.08	1890	2060	-8.6	-2.73	164	0.71626
	NL_CS	Surface (central)	6.8	3.6	1292	41	183	67	1318	622	47	0.1	2	0.06	1833	2034	-10.4	-2.88	174	0.71625
	NL_S3	Surface (margin)	6.8	3.6	1364	56	175	50	1498	456	44	0.1	2	0.07	1870	2042	-8.8	-3.14	171	0.71629
Discussion lake (69° 23' 21.27"S 76° 21' 07.24"E)	DL_S2	Surface margin	6.7	2.8	989	31	93	61	817	456	65	0.1	11	0.09	1328	1403	-5.5	-3.15	95	0.71298
	DL_CS	Surface central	6.5	3.0	919	33	100	54	910	289	70	0.2	12	0.09	1261	1340	-6.1	-3.59	91	0.71299
	DL_C2	2	6.7	2.7	990	30	92	46	854	456	76	0.2	12	0.06	1296	1461	-12.0	-3.27	100	0.71295
Lake L5 (69° 24' 27.63"S 76° 11' 03.36"E)	L5_S	Surface central	7.0	2.6	953	38	119	76	894	456	54	0.3	11	0.04	1382	1458	-5.4	-2.76	126	0.71344
	L5_5	5	6.9	2.9	880	29	107	69	987	289	54	0.3	9	0.07	1260	1385	-9.4	-3.09	131	0.71343
Sea Water	-	-	-	-	-	-	-	-	-	-	-	-	-	-	-	-	-	-	-	0.70921

Accepted Article

This article is protected by copyright. All rights reserved.

Table 2 *a-priori* values and associated uncertainties[a]

	Silicates[b,c,d]	Seawater,[e,f,g]	Carbonates[h]	Snow[i,j]
Cl/Na	0.01 ± 0.007	1.2 ± 0.006	0.01 ± 0.01	1.1 ± 0.09
Ca/Na	1.0 ± 0.2	0.02 ± 0.002	50 ± 20	0.1 ± 0.05
Mg/Na	2.1 ± 0.3	0.12 ± 0.0009	20 ± 8	0.1 ± 0.04
Sr/Na	2.7 ± 1.8	0.19 ± 0.008	80 ± 30	1.2 ± 0.9
$^{87}Sr/^{86}Sr$	0.82 ± 0.08	0.7092 ± 0	0.7090 ± 0.001	0.7097 ± 0.0007
Alk/Na	1.8 ± 0.4	0.01 ± 0.0001	100 ± 40	0.3 ± 0.22

[a]Uncertainties are in ±2σ, Sr/Na in nM/µM units.

[b]Sheraton et al. (1984), [c]Grew et al.(2013), [d]Maas et al. (2015)

[e]Carpenter and Manella (1973), [f]Veizer (1989), [g]Culkin and Cox (1966)

[h]Millot et al., (2003)

[i]Delmonte et al. (2013), [j]Grotti et al. (2015)

Accepted Article

This article is protected by copyright. All rights reserved.